FUDMA Journal of Engineering and Technology
ISSN: 3092-9385
https://fjet.fudutsinma.edu.ng/index.php/fjet/
Volume 2, Issue 2, 2026, 543-552

Spatial Scale Effects on the Relationship Between Land Use/Land Cover Change and Potential Evapotranspiration in Niger State, Nigeria

Muhammad M. ABDULLAHI[1*], Iyanda M. ANIMASHAUN[2], Ibrahim A. ABDULFATAI[3], George U. STEPHEN[4]

[1*]Ministry of Agriculture, Minna, Niger State, Nigeria
[1,2,4]Department of Agricultural and Bioresources Engineering, Federal University of Technology, Minna, Nigeria
[3]Department of Geology, Federal University of Technology, Minna, Nigeria

[1*]mmazhitu4u@gmail.com, [2]ai.iyanda@futminna.edu.ng, [3]a.asema@futminna.edu.ng, [4]stephengeorge022@gmail.com

Abstract
Potential evapotranspiration (PET) is a major climatic variable for irrigation planning, drought monitoring, and water-resources management, and its spatial distribution may be modified by land use/land cover (LULC) change. This study aimed to (i) quantify LULC changes in Niger State between 2004 and 2024, (ii) characterize the temporal and spatial patterns of PET, and (iii) determine whether the strength and direction of the LULC–PET relationship vary with spatial scale. Landsat 5 TM, Landsat 8 OLI, and Landsat 9 OLI-2 imagery were classified at 30 m using supervised Maximum Likelihood Classification for six LULC classes. PET was estimated with the Hargreaves method from Climate Research Unit climate inputs. An analytical dataset comprising 500 grid cells and three observation years (1,500 observations) was analysed at grid-cell, Local Government Area (LGA), and state-wide scales using percentage-change analysis, Pearson correlation, t-tests/ANOVA, and Mann–Kendall and Sen's slope trend tests. Grassland increased to 74.51% of the state by 2024, while built-up area increased from 0.19% to 1.14%. At grid-cell scale, PET was positively correlated with Forest ($r = 0.83$) and Cropland ($r = 0.74$), but negatively correlated with Built-up Area ($r = -0.70$), Grassland ($r = -0.64$), and Waterbody ($r = -0.58$). State-wide mean annual PET changed by only 0.52% and did not differ significantly among the three observation years ($p > 0.05$), although spatial variability increased. The results demonstrate a scale-dependent LULC–PET relationship and indicate that grid-cell and LGA-scale evidence is more informative for localized irrigation, drainage, land-use, and climate-adaptation decisions than state-wide averages.

Keywords: *Potential Evapotranspiration (PET), Land Use/Land Cover Change (LULC), Scale-Dependence, Guinea Savanna, Niger State.*

1.0 Introduction

Water is among the most critical natural resources sustaining agricultural production, ecosystem functioning, and socioeconomic development. Evapotranspiration governs how this resource moves between the land surface and the atmosphere. Potential evapotranspiration (PET), the maximum amount of water that could be lost to the atmosphere given unlimited moisture availability, is a key climatic variable underpinning irrigation planning, drought monitoring, and water resources management [1]. Climatic drivers such as temperature, radiation, humidity, and wind speed have traditionally been regarded as the principal controls on PET, but a growing body of evidence shows that land use/land cover (LULC) change also shapes evapotranspiration, by altering surface albedo, aerodynamic roughness, vegetation structure, and soil moisture availability [2-3].

Across Nigeria, rapid agricultural expansion, urbanization, deforestation, and infrastructural development have driven substantial and continuing transformation of the landscape [4-5]. These pressures are especially pronounced within the Guinea Savanna ecological zone, a transitional belt of tall grasses, scattered woodland, and a mosaic of natural and human-modified land covers that is highly sensitive to both climatic variability and anthropogenic disturbance. Studies elsewhere in West Africa's Guinea savanna have documented extensive and dynamic LULC turnover, including losses of woodland and savanna vegetation that outpace gains, driven by agricultural intensification, fuelwood extraction, and settlement growth [6]. Vegetation structure, rooting depth, and canopy characteristics differ markedly among savanna land cover types, so such transformations carry direct implications for the surface energy balance and, in turn, for evapotranspiration.

Niger State, located within the Guinea Savanna–Sudan Savanna transition zone of north-central Nigeria, experiences significant environmental and anthropogenic pressures. The state contains extensive croplands, forest reserves, grasslands, wetlands, and rapidly expanding urban areas. Over the past two decades, population growth, agricultural expansion, urbanization, and infrastructural development have substantially altered the distribution of major land use and land cover (LULC) classes. These changes can influence surface temperature, soil moisture, evapotranspiration, infiltration, and the overall surface water balance, thereby affecting potential evapotranspiration (PET).

Received: 25/08/2026; Revised: 31/08/2026; Accepted: 01/09/2026; Published: 10/09/2026

Understanding the relationship between LULC changes and PET is particularly important because variations in atmospheric water demand can influence crop water requirements, irrigation needs, soil-water availability, and agricultural productivity. Assessing these interactions can therefore support effective water-resources planning, irrigation scheduling, land-management decisions, drought-risk assessment, and climate-change adaptation in Niger State.

A persistent limitation in the literature is that the LULC-PET relationship is rarely examined as a function of spatial scale. Most existing assessments, in Nigeria and elsewhere, report a single, state- or basin-wide correlation between land cover proportions and evapotranspiration, treating the relationship as scale-invariant by default. Yet evidence from remote sensing and ecohydrological research indicates that the strength, and even the sign, of land surface-evapotranspiration relationships can shift markedly with the spatial resolution or aggregation unit of analysis. Studies applying energy-balance models across multiple satellite resolutions have shown that scale aggregation systematically alters the surface parameters that drive evapotranspiration estimates, including the selection of "hot" and "cold" reference pixels, vegetation indices, and albedo, with resulting discrepancies that can exceed those attributable to land cover pattern itself [7]. Multi-scale analyses linking land cover composition to hydrological and ecosystem functions have found something similar: the explanatory power of individual land cover classes varies considerably between fine-grained and coarser spatial units, so relationships detected at one scale may weaken, disappear, or even reverse at another. This is the modifiable areal unit problem, well documented in landscape-hydrology research. Because grid-cell, sub-basin, and state-wide analyses aggregate heterogeneous savanna landscapes differently, a single scale of analysis risks masking important local dynamics, or overstating relationships that only hold at broad spatial extents.

This is particularly important in a heterogeneous savanna environment such as Niger State, where forest patches, croplands, grasslands, bare surfaces, and expanding built-up areas occur in close spatial proximity. Consequently, the relationship between built-up expansion and potential evapotranspiration (PET) may appear weak when assessed at the state-wide scale due to spatial averaging. However, this relationship could be considerably stronger and more spatially pronounced within individual grid cells or local government areas surrounding major urban centres such as Minna, Bida, Suleja, and Kontagora. Broad state-level statistics, conversely, may obscure genuine, spatially localized responses of PET to forest loss or cropland conversion that only show up at finer resolutions. Without an explicit, multi-scale treatment, land and water resource planning risks being guided by relationships that don't actually hold at the scale where management decisions get made.

Building on a broader spatiotemporal assessment of LULC and PET dynamics in Niger State between 2004 and 2024, which integrated Landsat-derived land cover classification, gridded PET data, and correlation, regression, and trend analyses, This study builds upon previous research by explicitly investigating how the relationship between LULC and PET varies across different spatial scales, ranging from individual grid cells to aggregated administrative and broader landscape units, it addresses a gap in the West African literature, where LULC and PET dynamics are frequently studied independently and at a single spatial scale, which limits both the methodological rigour and the practical relevance of findings for localized environmental planning [8-9].

The present study therefore aims to examine the scale-dependent relationship between land use/land cover change and potential evapotranspiration in the Guinea Savanna ecosystem of Niger State, Nigeria, using satellite-derived LULC data and gridded PET estimates for 2004, 2014, and 2024. By comparing associations at multiple spatial scales, the study seeks to determine whether, and to what extent, the strength and direction of the LULC-PET relationship depend on the unit of analysis, providing more robust and scale-appropriate evidence to guide irrigation planning, land-use regulation, and climate adaptation strategies in Niger State and comparable savanna ecosystems across West Africa.

2. Materials and Methods

2.1 Description of the Study Area

Niger State is located in the north-central geopolitical zone of Nigeria, covering approximately 76,363 km² between latitudes 8°20'N–11°30'N and longitudes 3°30'E–7°20'E [10]. It is bordered by Zamfara and Kebbi States to the northwest and west, Kaduna State to the north, the Federal Capital Territory to the east, and Kogi and Kwara States to the south and southwest (Figure 1). The state straddles the transition between the Sudan Savanna in the north and the Guinea Savanna in the south, placing it within an ecologically heterogeneous belt that is highly responsive to both climatic variability and land surface change [11].

Relief is generally undulating, interspersed with inselbergs, river valleys, and the Shiroro Hills, while the Niger and Kaduna Rivers, together with the Kainji and Shiroro dams, form the backbone of the state's hydrology [12]. The climate is tropical continental, with a wet season from April to October and a Harmattan-influenced dry season from November to March. Mean annual rainfall ranges from about 1,100 mm in the north to over 1,600 mm in the south, and mean temperatures range from 25°C to 35°C [13]. Vegetation varies from relatively dense Guinea Savanna woodland and taller grasslands in the southern parts to more open and sparse Sudan Savanna vegetation toward the northern parts. [11], though this natural cover has been substantially modified by agriculture,

Received: 25/08/2026; Revised: 31/08/2026; Accepted: 01/09/2026; Published: 10/09/2026

fuelwood extraction, and urban growth around towns such as Minna, Bida, Suleja, and Kontagora [14]. These characteristics make Niger State a suitable setting for examining LULC–PET relationships in general, and specifically for testing whether such relationships hold consistently across spatial scales, given the fine-grained interspersion of cropland, forest, grassland, and built-up patches that typifies savanna transition landscapes.

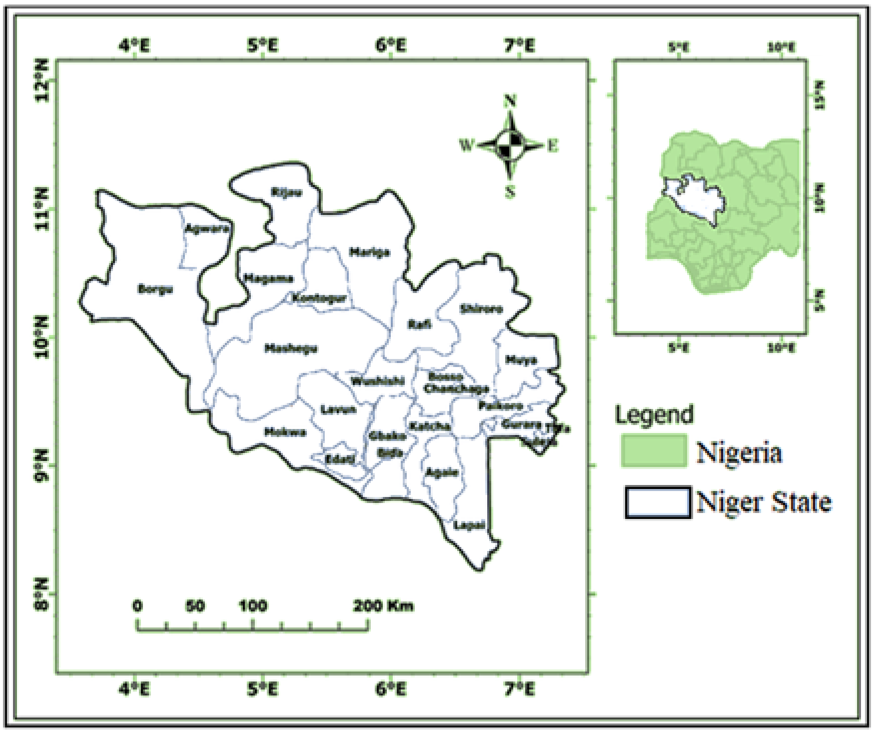

Figure. 1: The Study area

2.2 Data Sources

2.2.1 Land use/land cover data

LULC classification was based on Landsat imagery for 2004, 2014, and 2024, using Landsat 5 TM, Landsat 8 OLI, and Landsat 9 OLI-2 scenes at 30 m spatial resolution. Radiometric, atmospheric, and geometric corrections and cloud masking were applied before classification. Supervised Maximum Likelihood Classification was performed using training samples representing six classes: Bare Surface, Built-up Area, Cropland, Forest, Grassland, and Waterbody. NDVI was used as supporting spectral information for class separability. Post-classification comparison was used to quantify transitions between observation years. Classification accuracy was evaluated with a confusion matrix using reference observations/high-resolution imagery, and overall accuracy, producer's accuracy, user's accuracy, and the Kappa coefficient were reported following established remote-sensing accuracy assessment procedures [23]. For each class, area percentage was calculated as the class area divided by the total classified area, multiplied by 100.

$$ET_0 = 0.0023 \times R_a \times (Tmean + 17.8) \times (Tmax - Tmin)^{0.5} \quad [15\text{-}16]$$

2.2.2 Potential evapotranspiration data

Potential evapotranspiration (PET) was estimated using the Hargreaves temperature-based method [15-16]. The method was selected because it requires fewer meteorological variables than physically based methods such as Penman–Monteith. For each time step, mean, maximum, and minimum air temperatures were obtained from the Climate Research Unit (CRU) dataset, while extraterrestrial radiation was calculated from latitude and day of year following FAO-56 procedures [16]. The resulting PET estimates were aggregated to annual values and expressed in millimetres (mm).

R_a = extraterrestrial radiation calculated from latitude and day of year using the FAO-56 procedure [16].

where ET_0 is reference evapotranspiration (mm day^{-1}), Tmean is mean air temperature (°C), Tmax and Tmin are maximum and minimum air temperature (°C), respectively, and Ra is extraterrestrial radiation (MJ m^{-2} day^{-1}). The Hargreaves–Samani equation and the calculation of extraterrestrial radiation follow Hargreaves and Samani [15] and the FAO-56 procedures [16].

Received: 25/08/2026; Revised: 31/08/2026; Accepted: 01/09/2026; Published: 10/09/2026

2.2.3 Data Integration and Quality Control

An analytical database was constructed in Microsoft Excel by linking LULC percentages and PET values through a common Grid_ID and observation year. The database contained 500 spatial grid cells for 2004, 2014, and 2024, giving 1,500 grid-year observations. Quality control included completeness checks, verification that LULC percentages within each grid cell summed to approximately 100%, range checks for PET, box-and-whisker outlier screening in IBM SPSS Statistics v26, and exclusion of records that could not be recovered from the source datasets [17-18]. Derived variables included Dominant LULC, Urban Category, Vegetation Type, Forest Cropland Ratio, and Conversion Intensity.

2.2.4 Multi-Scale Analytical Framework

The strength, and even the direction, of land cover-hydrology relationships can shift with the spatial unit of analysis. This pattern is documented as the modifiable areal unit problem in landscape ecology and is increasingly reported in multi-scale ecosystem-service and land-cover studies [19-20]. For that reason, the LULC–PET relationship in this study was examined at three nested spatial scales rather than a single aggregation level:

a. Grid-cell scale. The finest unit of analysis, using the 500 individual 30 m-resolution grid cells directly capturing local heterogeneity in land cover composition and PET.
b. Local Government Area (LGA) scale. Grid cells were aggregated by zonal statistics to the 25 LGAs of Niger State, averaging LULC percentages and PET values within each administrative unit. This intermediate scale reflects the level at which land-use planning and water resource decisions are typically made.
c. State-wide scale. All grid cells were pooled into a single state-wide mean for each study year, representing the broadest level of aggregation and corresponding to the scale used in most prior LULC–PET assessments.

At each scale, Pearson correlation coefficients between PET and each LULC class (Bare Surface, Built-up Area, Cropland, Forest, Grassland, Waterbody) were computed independently, and the resulting correlation matrices were compared across scales to assess whether relationships strengthened, weakened, or reversed sign with increasing aggregation. This mirrors the approach used in multi-scale studies linking land cover composition to hydrological and ecosystem functions, where the explanatory power of individual land cover classes has been shown to vary considerably between fine-grained and coarser spatial units [21]. Zonal statistics and map algebra operations were carried out in a GIS environment to generate the LGA-level aggregates, with all datasets standardized to a common spatial resolution and projection prior to aggregation to ensure comparability.

2.2.5 Statistical Methods

Descriptive statistics were used to summarize LULC and PET at each spatial scale and observation year. Percentage change was calculated as:

% Change = $((\text{Value}_2 - \text{Value}_1) / \text{Value}_1) \times 100$ [adapted from standard percentage-change formulation]

Pearson product–moment correlation was used to quantify the linear association between PET and each LULC class. Independent-samples t-tests compared PET between two LULC-based groups, while one-way ANOVA followed by Tukey's HSD test compared PET among three or more groups. Statistical significance was evaluated at $\alpha = 0.05$. The Conversion Intensity Index (CII) was calculated as the cumulative absolute percentage change across the six LULC classes between 2004 and 2024; thresholds were defined using the Jenks Natural Breaks method. Long-term PET trends for 1970–2024 were evaluated with the Mann–Kendall test, and Sen's slope was used to estimate the magnitude of monotonic change [22].

Long-term trends in evapotranspiration were assessed using the Mann–Kendall trend test and Sen's slope estimator, following [22], to determine the presence, direction, and magnitude of monotonic trends independent of the LULC-scale comparison. Classification accuracy of the LULC maps was assessed using a confusion matrix derived from ground reference and high-resolution imagery, reporting overall accuracy, producer's and user's accuracy, and the Kappa coefficient [23].

Microsoft Excel 2024 served as the primary platform for database management, descriptive statistics, and change calculations. IBM SPSS Statistics v26 was used for outlier detection, correlation, regression, and comparative tests. ArcGIS 10.5 supported LULC classification, zonal aggregation to the LGA scale, and spatial visualization of PET and LULC patterns across scales.

3. Results and Discussion

3.1 Land Use/Land Cover Dynamics in Niger State (2004–2024)

Table 1 shows the LULC composition for 2004, 2014, and 2024. In 2004, Bare Surface represented 42.11% of the mapped area, followed by Grassland (34.39%) and Cropland (12.14%). By 2014, Grassland had increased to 54.15% and Cropland to 25.68%, while Bare Surface declined sharply to 0.02%. By 2024, Grassland had increased further to 74.51%, while Cropland declined to 12.82% and Forest to 8.73%. Built-up Area increased progressively from 0.19% in 2004 to 0.60% in 2014 and 1.14% in 2024. Waterbody also increased from 1.44% to

Received: 25/08/2026; Revised: 31/08/2026; Accepted: 01/09/2026; Published: 10/09/2026

2.76%. The continuous increase in grassland and built-up land is consistent with reported savanna degradation and peri-urban expansion in West Africa and sub-Saharan Africa [24-25]. See Table 1.

Table 1: Composition of the LULC classes across the three observation years.

LULC Class	2004 (%)	2014 (%)	2024 (%)	Overall Change 2004–2024 (%)
Bare Surface	42.11	0.02	0.05	−99.89
Built-up Area	0.19	0.60	1.14	+485.74
Cropland	12.14	25.68	12.82	+5.66
Forest	9.73	17.37	8.73	−10.27
Grassland	34.39	54.15	74.51	+116.68
Waterbody	1.44	2.18	2.76	+91.04

The pronounced 2004–2014 reduction in Bare Surface and the 2014 peak in Cropland and Forest should, however, be interpreted cautiously. Differences in image-acquisition season can alter the spectral appearance of senescent grass and actively growing vegetation, producing apparent changes that are partly classificational rather than physical [23-26]. Accordingly, Built-up Area and Waterbody, which changed monotonically across all three dates, provide more defensible indicators of directional land-cover change. This limitation is important when interpreting the subsequent fine-scale correlations because classification artefacts can propagate into derived LULC percentages.

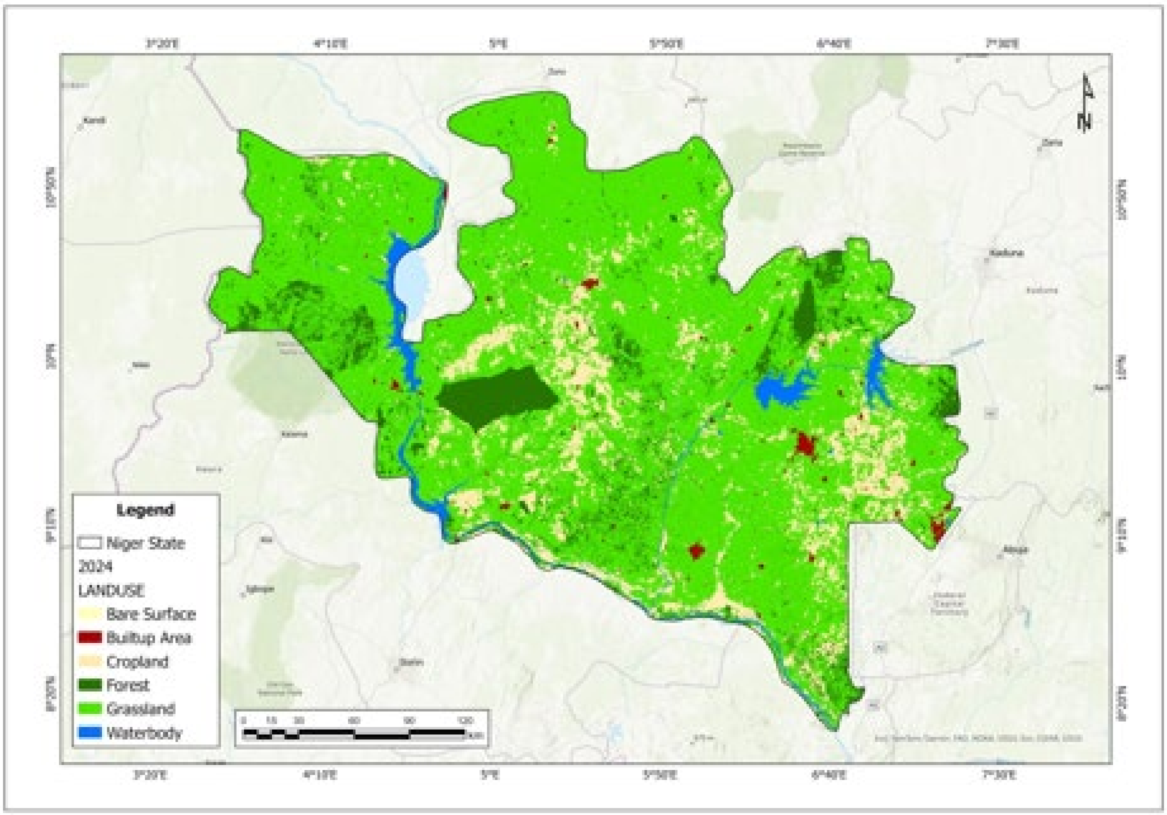

Figure. 2: LULC Map of Niger State (2024)

3.2 Temporal and Spatial Patterns in Potential Evapotranspiration

3.2.1 Temporal trend (state-wide scale).

Table 2 presents the state-wide PET statistics in chronological order. Mean annual PET increased slightly from 1631.7 mm in 2004 to 1636.4 mm in 2014, before declining to 1623.2 mm in 2024; the net change over 2004–2024 was only 0.52%. ANOVA indicated no statistically significant difference among the observation years ($p > 0.05$). In contrast, spatial variability increased progressively: the standard deviation rose from 9.8 mm in 2004 to 19.1 mm in 2014 and 24.0 mm in 2024, while the coefficient of variation increased from 0.6% to 1.4%. The stable mean alongside increasing dispersion indicates that PET demand became more spatially heterogeneous even though the state-wide average changed little. This finding agrees with studies emphasizing the dominant influence of climatic variables on regional evapotranspiration while recognizing that land cover modifies local surface-energy partitioning [16-27-28]. Similar averaging effects have been described in spatial analyses where heterogeneous local relationships become muted after aggregation [29]. See Table 2.

Table 2: Descriptive statistics of state-wide mean annual PET

Year	Mean (mm)	Min (mm)	Max (mm)	SD (mm)	CV (%)
2004	1631.7	1614.5	1645.6	9.8	0.6
2014	1636.4	1613.3	1666.5	19.1	1.1
2024	1623.2	1586.0	1658.7	24.0	1.4

3.2.2 Spatial pattern (intermediate, LGA scale)

Table 3 shows that the LGA-scale PET pattern was relatively persistent across the three decades. During 1995–2004, high mean PET occurred in Kontagora (1898.4 mm), Mokwa (1883.1 mm), and Rafi (1882.1 mm), whereas Gurara (1322.7 mm), Gbako (1362.1 mm), and Bida (1368.2 mm) were among the lower-PET LGAs. During 2005–2014, the broad spatial ordering remained similar, with Kontagora (1904.6 mm), Rafi (1892.3 mm), and Mokwa (1886.3 mm) remaining high and Gurara (1329.6 mm) and Gbako (1368.6 mm) remaining comparatively low. During 2015–2024, Mokwa (1882.4 mm), Rafi (1880.3 mm), and Kontagora (1895.9 mm) continued to show high mean PET, while Gurara (1319.2 mm), Rijau (1364.8 mm), and Bida (1383.1 mm) remained comparatively lower. The persistence of this spatial hierarchy suggests that broad climatic gradients exert a strong control at the LGA scale, with LULC effects superimposed locally. This interpretation is consistent with regional evidence that temperature and radiation gradients influence evaporative demand across savanna enviro nments [30]. See Table 3

Table 3: Inter-decadal statistics of PET at LGA scale in Niger State

	1995-2004			2005-2014			2015-2024		
	Mean	StDev	CV (%)	Mean	StDev	CV (%)	Mean	StDev	CV (%)
Bida	1368.2	11.4	0.8	1374.2	18.8	1.3	1383.1	20.5	1.4
Gbako	1362.1	11.2	0.8	1368.6	16.5	1.1	1382.4	20.4	1.4
Lapai	1812.1	7.7	0.4	1814.4	18.1	0.9	1805.4	29.6	1.6
Mokwa	1883.1	13.3	0.7	1886.3	17.1	0.9	1882.4	25.3	1.3
Agwara	1455.4	16.7	1.1	1460.9	20.7	1.3	1437.7	40.1	2.6
Kontagora	1898.4	10.5	0.5	1904.6	19.1	1.0	1895.9	28.1	1.4
Rijau	1456.5	17.9	1.2	1448.8	45.7	3.0	1364.8	32.7	2.3
Wushishi	1379.1	12.2	0.8	1388.3	21.3	1.5	1388.5	22.5	1.5
Gurara	1322.7	9.1	0.7	1329.6	20.0	1.4	1319.2	24.3	1.7
Minna	1826.6	7.7	0.4	1834.0	21.5	1.1	1823.8	31.3	1.6
Paiko	1812.1	7.7	0.4	1814.4	18.1	0.9	1789.1	40.6	2.2
Rafi	1882.1	7.6	0.4	1892.3	22.6	1.1	1880.3	32.0	1.6
Shiroro	1826.6	7.7	0.4	1834.0	21.5	1.1	1823.8	31.3	1.6
Suleja	1778.3	6.7	0.4	1781.0	18.6	1.0	1770.1	29.8	1.6

3.2.3 Grid-Cell (Fine) Scale Relationship between LULC and PET

Table 4 presents the pooled Pearson correlation matrix for the 1,500 grid-year observations. PET showed strong positive correlations with Forest ($r = 0.83$) and Cropland ($r = 0.74$), while correlations were negative with Built-up Area ($r = -0.70$), Grassland ($r = -0.64$), and Waterbody ($r = -0.58$). [31-32]. The negative Built-up–PET relationship is consistent with the reduction in vegetated and permeable surfaces associated with urbanization and changes in the partitioning of available energy [33-34]. The negative Grassland association should be interpreted in the context of the study's mapped land-cover composition and the strong correlations among LULC classes rather than as evidence that grassland intrinsically suppresses PET under all conditions [35]. See Table 4

Table 4: Pearson correlation matrix between LULC classes and PET (n = 1,500)

	Bare Surface	Built-up	Cropland	Forest	Grassland	Waterbody	PET
Bare Surface	1						
Built-up	−0.82	1					
Cropland	−0.54	−0.03	1				
Forest	−0.41	−0.18	0.99	1			
Grassland	−0.86	0.99	0.04	−0.11	1		
Waterbody	−0.90	0.99	0.11	−0.04	0.99	1	
PET	0.17	**−0.70**	**0.74**	**0.83**	**−0.64**	**−0.58**	1

Received: 25/08/2026; Revised: 31/08/2026; Accepted: 01/09/2026; Published: 10/09/2026

The LULC predictors themselves were highly intercorrelated; for example, Built-up Area, Grassland, and Waterbody showed pairwise correlations of approximately 0.99 in the pooled grid dataset. This indicates strong compositional dependence among percentage-based LULC variables and warns against interpreting individual correlation coefficients as independent causal effects. Any future multivariable regression should therefore assess multicollinearity using variance inflation factors before interpreting regression coefficients [36].

The contrast between the fine and broad scales is the central finding. At the grid-cell scale, PET showed strong associations with several LULC classes, with $|r|$ reaching 0.83. However, the same period produced only a 0.52% change in state-wide mean PET despite nearly fivefold built-up growth and more than doubling of grassland share. This attenuation after aggregation is consistent with multi-scale research showing that relationships between land cover and environmental functions can weaken, change magnitude, or change the dominant explanatory variable as the spatial unit becomes coarser [7-19-21] further showed that spatial aggregation can affect the surface parameters used in satellite-based evapotranspiration estimation. Thus, the weak state-wide signal should not be interpreted as evidence of an absence of local LULC influence; it indicates that heterogeneous local effects are partly averaged out.

At the LGA scale, the persistence of relatively high- and low-PET areas between periods suggests an intermediate response. Minna, Shiroro, Rafi, and Mokwa remained among the higher-demand areas, whereas Gurara, Wushishi, Gbako/Bida, and Rijau were generally lower. The stability of these zones despite local LULC turnover supports the interpretation that climatic gradients dominate the broad LGA signature, while land-cover differences contribute to within-LGA variation. This intermediate pattern links the strong fine-scale associations to the muted state-wide mean.

1.3 Long-Term Trend Analysis of Potential Evapotranspiration (1970–2024)

Table 5 summarizes the 1970–2024 Mann–Kendall and Sen's slope results. Statistically significant increasing trends were detected for Bida ($Z = 3.66$, $p < 0.001$), Gbako ($Z = 4.68$, $p < 0.001$), Mokwa ($Z = 2.81$, $p < 0.01$), Kontagora ($Z = 2.81$, $p < 0.01$), Rafi ($Z = 2.62$, $p < 0.01$), Lapai ($Z = 2.05$, $p < 0.05$), Wushishi ($Z = 2.39$, $p < 0.05$), Minna ($Z = 2.07$, $p < 0.05$), and Shiroro ($Z = 2.07$, $p < 0.05$). Rijau showed a significant decreasing trend ($Z = -2.69$, $p < 0.01$), whereas Agwara, Gurara, and Paiko did not show statistically significant trends at $\alpha = 0.05$. These long-term results complement the 2004–2024 spatial comparison: short-period state-wide means may remain stable even when the longer climate record shows significant monotonic trends in individual areas. Earlier analysis by [37] also reported significant increases in evapotranspiration during March, April, May, November, and the dry season overall. The agreement supports the interpretation that climatic forcing has increased evaporative demand over parts of Niger State, while the fine-scale LULC associations represent an additional spatial modulation of PET. Regional evidence of increasing evaporative demand under warming conditions in West Africa provides further context for this result [30-38]. See Table 5.

Table 5: Mann–Kendall trend statistics and Sen's slope estimates of PET for areas within Niger State (1970–2024)

Time series	Mean	StDev	Test Z	Q
Bida	1366.6	22	3.66***	0.732
Gbako	1359.0	24	4.68***	0.932
Lapai	1802.9	26	2.05*	0.459
Mokwa	1873.1	28	2.81**	0.719
Agwara	1446.0	27	1.28	0.332
Kontagora	1888.9	28	2.81**	0.711
Rijau	1431.0	44	-2.69**	-1.146
Wushishi	1378.6	22	2.39*	0.539
Gurara	1318.5	21	1.61	0.283
Minna	1820.2	27	2.07*	0.479
Paiko	1799.9	29	1.22	0.278
Rafi	1874.0	29	2.62**	0.669
Shiroro	1820.2	27	2.07*	0.479
Suleja	1769.0	25	1.85+	0.359

Note: *** indicates statistical significance at $\alpha = 0.001$; ** at $\alpha = 0.01$; * at $\alpha = 0.05$.

The results across the three spatial scales provide a coherent chronological interpretation. First, the 2004–2024 LULC record shows substantial landscape transformation, most reliably expressed by continuous grassland expansion and continuous built-up growth (Table 1). Second, the PET observations show that the state-wide mean

Received: 25/08/2026; Revised: 31/08/2026; Accepted: 01/09/2026; Published: 10/09/2026

remained relatively stable from 2004 to 2024, while spatial dispersion increased (Table 2). Third, the LGA results demonstrate that the geography of relatively high- and low-PET zones persisted across the observation periods (Table 3). Finally, the fine-scale correlation analysis shows that individual LULC classes were strongly associated with PET (Table 4), whereas aggregation to the state level substantially weakened the apparent relationship. This scale gradient is consistent with the modifiable areal unit problem and with previous multi-scale studies showing that aggregation can weaken or alter observed land-cover–environment relationships [19-21]. The independent 1970–2024 trend analysis further indicates that climatic forcing has contributed to increasing evaporative demand in several LGAs, particularly during the dry-season months reported previously for Niger State [37]. Taken together, the findings suggest that climate and land cover operate simultaneously but become visible at different spatial and temporal scales. Therefore, state-wide PET stability should not be interpreted as evidence that LULC change has no local effect; rather, the strong grid-level associations indicate localized land-surface controls that are masked by spatial aggregation.

4.Conclusion

This study determined the relationship between land use/land cover change and potential evapotranspiration in the Guinea Savanna ecosystem of Niger State. Between 2004 and 2024, grassland expanded to 74.51% of the state and built-up area increased from 0.19% to 1.14%. At the grid-cell scale, PET was strongly positively associated with Forest and Cropland and negatively associated with Built-up Area, Grassland, and Waterbody. At the state-wide scale, mean annual PET changed by only 0.52% and showed no statistically significant inter-annual difference, although its spatial variability increased substantially. The LGA scale showed a persistent spatial hierarchy of relatively high- and low-PET zones. These results demonstrate that the observed LULC–PET relationship depends strongly on the spatial unit of analysis.

From a management perspective, the results support the use of grid-cell and LGA-level information for localized irrigation scheduling, drainage planning, land-use regulation, and climate adaptation, while state-wide averages remain useful for regional water-balance planning. The study also identifies an important limitation: the unusually large changes in Bare Surface, Cropland, and Forest may partly reflect differences in Landsat image-acquisition season and associated classification effects. Future research should therefore use seasonally matched imagery, report formal LGA-level correlation statistics from the underlying grid database, and incorporate additional climatic controls where available. Such improvements would strengthen attribution of PET changes between climatic forcing and land-cover transformation.

References

[1] N. Bjarke, J. Barsugli, & B. Livneh, . Ensemble of CMIP6 derived reference and potential evapotranspiration with radiative and advective components. *Sci Data* **10**, 417 (2023). https://doi.org/10.1038/s41597-023-02290-0

[2] K. O. Babaremu, O. Taiwo, and D. Ajayi, “Impacts of land use and land cover changes on hydrological response: A review of current understanding and implications for watershed and water resources management,” 2024.

[3] H. Wang, J. Chen, Y. Liu, and X. Zhao, “Land cover change impacts on evapotranspiration dynamics and water balance: Evidence from multi-temporal remote sensing observations,” Remote Sensing of Environment, vol. 315, p. 114382, 2024.

[4] O. M. Alegbeleye, O. S. Adesina, and O. A. Oladipo, “Land use land cover analysis in Nigeria: A systematic review of data, methods and platforms with future prospects,” Bulletin of the National Research Centre, vol. 48, no. 1, pp. 1–23, 2024.

[5] O. O. Agumagu, R. Marchant, and L. C. Stringer, "Land use and land cover change dynamics in the Niger Delta region of Nigeria from 1986 to 2024," *Land*, vol. 14, no. 4, p. 765, 2025. doi: 10.3390/land14040765.

[6] K. S. Dahan, R. A. Kasei, and R. Husseini, “Land use land cover (LULC) degradation intensity analysis of Guinea savannah and mosaic forest savannah zones in Ghana,” All Earth, vol. 35, no. 1, pp. 302–328, 2023.

[7] X. Li, X. Xu, X. Wang, S. Xu, W. Tian, J. Tian, and C. He, “Assessing the effects of spatial scales on regional evapotranspiration estimation by the SEBAL model and multiple satellite datasets: A case study In the agro-pastoral ecotone, northwestern China,” Remote Sensing, vol. 13, no. 8, p. 1524, 2021.

[8] F. Akinyemi, M. Bello, and R. Yusuf, “Remote sensing assessment of land surface temperature and evapotranspiration trends in northern Nigeria,” Journal of Arid Environments, vol. 209, p. 104889, 2023.

[9] A. J. Oloruntade and B. Adeyemi, “Impacts of agricultural expansion on evapotranspiration in the Nigerian savannah,” Agricultural Water Management, vol. 260, p. 107310, 2022.

[10] Niger State Government, “About Niger State: Official state profile and geography,” 2024.

[11] A. G. Ojanuga, The Soils and Agroecological Zones of Nigeria. Federal Ministry of Agriculture and Rural Development, 2006.

[12] FAO AQUASTAT, “Nigeria water resources profile,” Food and Agriculture Organization, 2021.
[13] Nigeria Meteorological Agency (NiMet), “Climate data normals and agroclimatic advisory for north-central Nigeria,” Abuja, Nigeria, 2023.
[14] National Bureau of Statistics (NBS), “Niger State statistical fact sheet,” Abuja, Nigeria, 2022.
[15] G. H. Hargreaves and Z. A. Samani, “Reference crop evapotranspiration from temperature,” Applied Engineering in Agriculture, vol. 1, no. 2, pp. 96–99, 1985.
[16] R. G. Allen, L. S. Pereira, D. Raes, and M. Smith, Crop Evapotranspiration: Guidelines for Computing Crop Water Requirements, FAO Irrigation and Drainage Paper No. 56. Rome, Italy: FAO, 1998.
[17] A. Field, Discovering Statistics Using IBM SPSS Statistics, 5th ed. London, U.K.: Sage, 2018.
[18] D. C. Montgomery and G. C. Runger, Applied Statistics and Probability for Engineers, 7th ed. Hoboken, NJ, USA: Wiley, 2018.
[19] L. Ding, Y. Liao, C. Zhu, Q. Zheng, and K. Wang, “Multiscale analysis of the effects of landscape pattern on the trade-offs and synergies of ecosystem services in southern Zhejiang Province, China,” Land, vol. 12, no. 5, p. 949, 2023.
20] Z. Lv, B. Wang, Z. Zhen, and J. Wang, “Multi-scale spatiotemporal trade-offs and synergies of ecosystem services: Implications for zoned ecological governance in the Shanxi section of the Yellow River Basin,” Frontiers in Environmental Science, vol. 14, p. 1890546, 2026.
[21] S. Li, S. Peng, B. Jin, J. Zhou, and Y. Li, “Multi-scale relationship between land use/land cover types and water quality in different pollution source areas in Fuxian Lake Basin,” PeerJ, vol. 7, p. e7283, 2019.
[22] I. M. Animashaun, P. G. Oguntunde, O. O. Olubanjo, and A. S. Akinwumiju, "Analysis of variations and trends of temperature over Niger central hydrological area, Nigeria, 1911–2015," *Physics and Chemistry of t he Earth, Parts A/B/C*, vol. 131, p. 103445, 2023. doi: 10.1016/j.pce.2023.103445.
[23] R. G. Congalton and K. Green, Assessing the Accuracy of Remotely Sensed Data: Principles and Practices, 3rd ed. Boca Raton, FL, USA: CRC Press, 2019.
[24] United Nations Human Settlements Programme (UN-Habitat), World Cities Report 2022: Envisaging the Future of Cities. Nairobi, Kenya: UN-Habitat, 2022.
[25] A. O. Arowolo, X. Deng, O. A. Olatunji, and A. E. Obayelu, “Assessing changes in the pattern of land use and land cover over time and projected future changes using CA-Markov model in Nigeria,” Sustainability, vol. 10, no. 10, p. 3572, 2018.
[26] D. Lu, P. Mausel, E. Brondízio, and E. Moran, “Change detection techniques,” International Journal of Remote Sensing, vol. 25, no. 12, pp. 2365–2401, 2019.
[27] T . R. McVicar, M. L. Roderick, R. J. Donohue, L. T. Li, T. G. Van Niel, A. Thomas, J. Grieser, D. Jhajharia, Y. Himri, N. M. Mahowald, A. V. Mescherskaya, A. C. Kruger, S. Rehman, and Y. Dinpashoh, “Global review and synthesis of trends in observed terrestrial near-surface wind speeds: Implications for evaporation,” Journal of Hydrology, vol. 416–417, pp. 182–205, 2012.
[28] J. B. Fisher, F. Melton, E. Middleton, C. Hain, M. Anderson, R. Allen, M. F. McCabe, S. Hook, R. Baldocchi, P. A. Townsend, A. Kilic, K. Tu, D. G. Miralles, J. P. Perret, J. P. Lagouarde, D. Waliser, A. J. Purdy, A. French, D. Schimel, and E. F. Wood, “The future of evapotranspiration: Global requirements for ecosystem functioning, carbon and climate feedbacks, agricultural management, and water resources,” Water Resources Research, vol. 53, no. 4, pp. 2618–2626, 2017.
[29] S. Openshaw, The Modifiable Areal Unit Problem, Concepts and Techniques in Modern Geography 38. Norwich, U.K.: GeoBooks, 1984.
[30] M. B. Sylla, P. M. Nikiema, P. Gibba, I. Kebe, and N. A. B. Klutse, “Climate change over West Africa: Recent trends and future projections,” in Adaptation to Climate Change and Variability in Rural West Africa, V. R. Singh, Ed. Cham, Switzerland: Springer, 2018, pp. 25–40.
[31] G. B. Bonan, “Forests and climate change: Forcings, feedbacks, and the climate benefits of forests,” Science, vol. 320, no. 5882, pp. 1444–1449, 2008.
[32] X. Li, Y. Zhang, G. Sun, and S. Wang, “Impacts of land use and land cover change on evapotranspiration and regional hydrological processes,” Journal of Hydrology, vol. 624, p. 129846, 2023.
[33] Giardina, F., Gentine, P., Konings, A. G., Seneviratne, S. I., & Stocker, B. D. (2023). Diagnosing evapotranspiration responses to water deficit across biomes using deep learning. *New Phytologist*, *240*(3), 968-983.
[34] T. R. Oke, “The energetic basis of the urban heat island,” Quarterly Journal of the Royal Meteorological Society, vol. 108, no. 455, pp. 1–24, 1982.
[35] Y. Zhang, X. Xiao, C. Jin, S. Zhou, and S. C. Wofsy, “Vegetation change and evapotranspiration responses across diverse ecosystems under changing environmental conditions,” Global Change Biology, vol. 28, no. 12, pp. 3742–3758, 2022.
[36] J. F. Hair, W. C. Black, B. J. Babin, and R. E. Anderson, Multivariate Data Analysis, 8th ed. Andover, U.K.: Cengage Learning, 2019.

[37] M. M. Abdullahi, I. M. Animashaun, and I. A. Abdulfatai, "Variability and trend analysis of evapotranspiration over Niger State, Nigeria," in Proceedings of the 4th College of Engineering International Conference (CEIC 2026), Federal University of Agriculture, Abeokuta, Nigeria, Apr. 28–30, 2026, pp. 6–14.
[38] H. Tabari, S. Marofi, A. Aeini, P. H. Talaee, and K. Mohammadi, "Trend analysis of reference evapotranspiration in the western half of Iran," Agricultural and Forest Meteorology, vol. 151, no. 2, pp. 128–136, 2011.
[39] B. Adeyemi, K. Ogunjobi, and M. Fasona, "Spatiotemporal variability of evapotranspiration in Nigeria using the Penman–Monteith approach," Climate and Development, vol. 13, no. 6, pp. 1–12, 2021.

Received: 25/08/2026; Revised: 31/08/2026; Accepted: 01/09/2026; Published: 10/09/2026